



HAL
open science

Neurospheres on Patterned PEDOT:PSS Microelectrode Arrays Enhance Electrophysiology Recordings

Jolien Pas, Charalampos Pitsalidis, Dimitrios Koutsouras, Pascale Quilichini, Francesca Santoro, Bianxiao Cui, Laurent Gallais, Rodney O'Connor, George Malliaras, Róisín Owens

► To cite this version:

Jolien Pas, Charalampos Pitsalidis, Dimitrios Koutsouras, Pascale Quilichini, Francesca Santoro, et al.. Neurospheres on Patterned PEDOT:PSS Microelectrode Arrays Enhance Electrophysiology Recordings. *Advanced Biosystems*, 2017, 2 (1), pp.1700164. 10.1002/adbi.201700164 . hal-03796171

HAL Id: hal-03796171

<https://amu.hal.science/hal-03796171>

Submitted on 4 Oct 2022

HAL is a multi-disciplinary open access archive for the deposit and dissemination of scientific research documents, whether they are published or not. The documents may come from teaching and research institutions in France or abroad, or from public or private research centers.

L'archive ouverte pluridisciplinaire **HAL**, est destinée au dépôt et à la diffusion de documents scientifiques de niveau recherche, publiés ou non, émanant des établissements d'enseignement et de recherche français ou étrangers, des laboratoires publics ou privés.

Neurospheres on Patterned PEDOT:PSS Microelectrode Arrays Enhance Electrophysiology Recordings

*Jolien Pas, Charalampos Pitsalidis, Dimitrios A. Koutsouras, Pascale P. Quilichini, Francesca Santoro, Bianxiao Cui, Laurent Gallais, Rodney P. O'Connor, George G. Malliaras, and Róisín M. Owens**

Microelectrode arrays (MEAs) are a versatile diagnostic tool to study neural networks. Culture of primary neurons on these platforms allows for extracellular recordings of action potentials. Despite many advances made in the technology to improve such recordings, the recording yield on MEAs remains sparse. Here, enhanced recording yield is shown induced by varying cell densities on poly(3,4-ethylenedioxythiophene):poly(styrenesulfonate)-coated MEAs. It is demonstrated that high cell densities (900 cells mm⁻²) of primary cortical cells increase the number of recording electrodes by 53.1% ± 11.3%, compared with low cell densities (500 cells mm⁻²) with 6.3% ± 1.4%. To further improve performance, 3D clusters known as neurospheres are cultured on the MEAs, significantly increasing single unit activity recordings. Extensive spike sorting is performed to analyze the unit activity recording multiple neurons with a single microelectrode. Finally, patterning of polyethylene glycol diacrylate through laser ablation is demonstrated, as a means to more precisely confine neurospheres on top of the electrodes. The possibility of recording single neurons with multiple neighboring electrodes is shown. Overall, a total recording yield of 21.4% is achieved, with more than 90% obtained from electrodes with neurospheres, maximizing the functionality of these planar MEAs as effective tools to study pharmacology-based effects on neural networks.

J. Pas, Dr. C. Pitsalidis, Dr. D. A. Koutsouras, Dr. R. P. O'Connor,
Prof. G. G. Malliaras, Prof. R. M. Owens
Department of Bioelectronics
Ecole Nationale Supérieure des Mines, CMP-EMSE
Gardanne 13541, France
E-mail: rmo37@cam.ac.uk

Dr. P. P. Quilichini
Aix Marseille Univ
INSERM, INS, Inst Neurosci Syst
Marseille 13005, France

Dr. F. Santoro, Prof. B. Cui
Department of Chemistry, Stanford University
Stanford, CA 94305, USA

Dr. F. Santoro
Center for Advanced Biomaterials for HealthCare
Italian Institute of Technology (IIT)
Naples 80125, Italy

Dr. L. Gallais
Aix Marseille Univ, CNRS, Centrale Marseille
Institut Fresnel

13397 Marseille Cedex 20, France

Prof. G. G. Malliaras,
Electrical Engineering Division, University of Cambridge
Cambridge CB3 0AS, UK

Dr. R. M. Owens
Department of Chemical Engineering and Biotechnology
University of Cambridge
Cambridge CB3 0FA, UK

1. Introduction

The brain is continuously processing electrochemically transduced information via an entangled yet organized network of billions of neurons. As the most complex organ in the human body, subtle changes in its structure and function can greatly affect the quality of life. Almost 2% of the total world's population suffers from neurological disorders, a number that is expected to grow substantially in the future.^[1] There is thus a great need to understand the nature of disorders of the central nervous system in general to diagnose them and develop therapies.

One way to systematically study the electrophysiology of neural systems is through in vitro recording of neural activity using microelectrode arrays (MEAs).^[2] MEAs provide a noninvasive way to record changes in the extracellular field generated by cells cultured on the device. The field potentials are caused by ionic current flow within the cell culture and include fast action potentials of individual neurons (i.e., unit activity), subthreshold synaptic potentials, and even slow glial potentials.^[3,4] The extracellular detection of those signals in vitro can be modeled using an electronic circuit (reviewed and detailed by Spira and Hai^[5]) and depends mostly on the magnitude, sign, and distance of the neurons from the electrode site.^[3,4] In a successful recording, the extracellular signal is in the range of tens to hundreds of microvolts and is measured within some milliseconds. In 1980, Pine was the first to report MEA recordings from dissociated neuronal cultures.^[6] Since then, this in vitro method has been widely explored, and a diverse catalogue of MEAs has been developed for different applications.^[2,4,5] Essential for in vitro recording are:

(1) an accurate and sensitive recording system and (2) an electrically active neural network. To this end, various device designs and neural cell culture optimizations have been explored to improve the success of microelectrode studies, as briefly described below.

On the device side, 2D and 3D designs have been investigated to improve electrical coupling between neurons and recording sites.^[4,5,7] Microelectrodes are typically made of metallic conductors, such as gold, titanium nitride, platinum, etc. Generally, the electrode size, number, and interelectrode spacing vary from 5 to 50, 32 to 60, and 100 to 250 μm , respectively.^[7] The recording performance of the microelectrodes can be improved by increasing their effective surface area by surface modification with nanostructures or other electrode coatings, thereby reducing the electrode impedance. Examples of such modifications include porous platinum black, golden nanoflakes or -pillars, carbon nanotubes, conducting polymers such as polypyrrole and poly(3,4-ethylenedioxythiophene):poly(styrenesulfonate) (PEDOT:PSS).^[7-11] To further improve MEA recordings, recent efforts have focused on creating 3D microelectrodes to interface intracellularly with cells.^[5] However, the main limitation of this approach is that long-term recording is not yet possible, most probably due to their invasive nature, as only multiple day experiments have been reported.

On the biology side, the culture of primary neural cells on top of MEAs remains a challenge. Most importantly, neurons need to survive for long periods on the substrates (preferentially several weeks), and they need to be as close as possible to the electrode site and within the recording distance ($<140 \mu\text{m}$).^[12] However, their tendency to adhere randomly to the substrate after cell seeding renders this rather challenging, unless there is a particular cell pattern designed on the device. Thus, a plethora of patterning techniques has been developed aiming to make the surface either cell adhesive and/or cell refractive, including microcontact printing, surface modifications, or the use of physical structures (reviewed by Kim et al.^[7]). The most commonly used coatings as cell adhesion

promoters on MEAs include collagen, poly-lysine and laminin.^[13] Notably, a primary cell culture contains multiple cell types apart from the neurons, such as astrocytes, oligodendrocytes, and microglia. While mature neurons do not undergo cell division, the other supporting cells in the brain (particularly astrocytes) do not have that restriction. Continuous proliferation and migration of astrocytes can push neurons away from the electrode site by positioning themselves below the neural somas.^[14] The presence of glial cells is nevertheless important for neuronal communication.^[15,16] The use of serum-free media can be a simple way to prevent overgrowth of glial cells in vitro.^[13] However, the growth of cells in vitro, being a rather dynamic process, can affect the performance of the microelectrodes due to the continuous deposition of proteins from the media and the extracellular matrix (ECM) of the cells resulting in the so-called biofouling of the microelectrodes within days.^[13]

Despite the abovementioned efforts to optimize in vitro MEA recordings, the overall recording yield of MEAs remains sparse.^[5,17] While the whole reason for developing MEAs is to record action potentials from multiple neurons simultaneously, the probability of recording such small signals is very low. This challenge is difficult to quantify, as numerous parameters play a role, including, for example, electrode density and surface treatment, the type of neurons and their cell density, etc. It is nevertheless a well-known problem in the in vitro neuroengineering field. Here, we demonstrate an enhancement of recording spontaneous single units through the formation of neurospheres on planar, custom-made MEAs. We initially found that a high cell density (HCD) on our PEDOT:PSS-coated MEAs significantly increased the number of recording electrodes. The presence of even higher local cell densities in the form of 3D clusters, known as neurospheres, further improved MEA recording performance. This more natural cellular organization of central nervous system cells in vitro increased the success rate of recording single unit activity per microelectrode to 42.2%. We demonstrate this through the analysis of multiple MEA recordings using semiautomated spike sorting algorithms. Finally, we demonstrate how to confine neurospheres on MEAs through laser patterning of polyethylene glycol diacrylate (PEGDA). This approach provides a way to control the location of neurospheres on the MEA to further maximize their recording yield.

2. Results and Discussion

2.1. MEA Design and Growth of Cortical Cells

Figure 1 a shows a PEDOT:PSS-coated MEA device fabricated on a glass substrate. The metal electrodes were patterned by photolithography and insulated with parylene C. Each MEA contains 64 electrodes, spaced 100 μm from center to center and with an active area of $12 \times 12 \mu\text{m}^2$ (Figure S1, Supporting Information). All the electrodes were coated with the conducting polymer PEDOT:PSS via a peel-off technique, as previously reported.^[9,11] The addition of the conducting polymer significantly lowered the impedance, resulting in an average impedance of $38.5 \pm 2.4 \text{ k}\Omega$ at 1 kHz. A glass well was placed around the electrode area and used as container of cell media. Prior to cell seeding, the MEA was coated with the polypeptide poly-D-lysine (PDL) and the ECM protein laminin, known to improve both cell adhesion and neurite outgrowth.^[16,18-20] Without any coating, cells did not survive past 5 days in vitro (DIV5) (Figure S2, Supporting Information).

Rat embryonic day 18 (E18) primary cortical cells grew a complex network within a couple of weeks in culture. The cells adhered within 1 h on the MEAs and as shown in the scanning

electron microscopy (SEM) images, they also attached to the PEDOT:PSS-coated microelectrodes (Figure 1b,c). The images show the top (Figure 1b) and cross-sectional (Figure 1c) view of a microelectrode with a single cell on top (indicated in blue) and a complex network of neurites and ECM around. The cross-section was performed as presented in ref. [21] using a focused ion beam (FIB) prepared sample (see Experimental Section). The image demonstrates the coverage of PEDOT:PSS on gold, the encapsulation of parylene around it and most importantly, the tight attachment of the cell on the microelectrode. The development of a complex network of neurites within three weeks of culture is shown in Figure 1d. After DIV21, the number of synapses at the dendrites and soma is known to have reached saturation.^[4] Recording of spontaneous activity was consequently performed after DIV21.

The presence of neurons and astrocytes in the cell culture was

2.2. Comparison of low versus High Cell Densities

The differences in recording yield between MEAs seeded with a low cell density (500 cells mm⁻², LCD) and a HCD (900 cells mm⁻²) were compared. **Figure 2a** shows phase contrast images and scatter plots based on a principal component analysis (PCA) of the two different cell density experimental groups. The scatter plots show a 2D view of the sorted single units done via the PCA (see Experimental Section). The classification of units is based on spike amplitude and waveform variability within the recorded electrophysiological data.^[23,24] In short, data recorded from one electrode can contain single unit activity from multiple neurons. Identified units were isolated from the data, and classical techniques of spike sorting were used to group the recorded spikes into individual neurons, called "clusters."^[23,25] Each unit cluster (i.e., activity originating from one given neuron) is subsequently shown

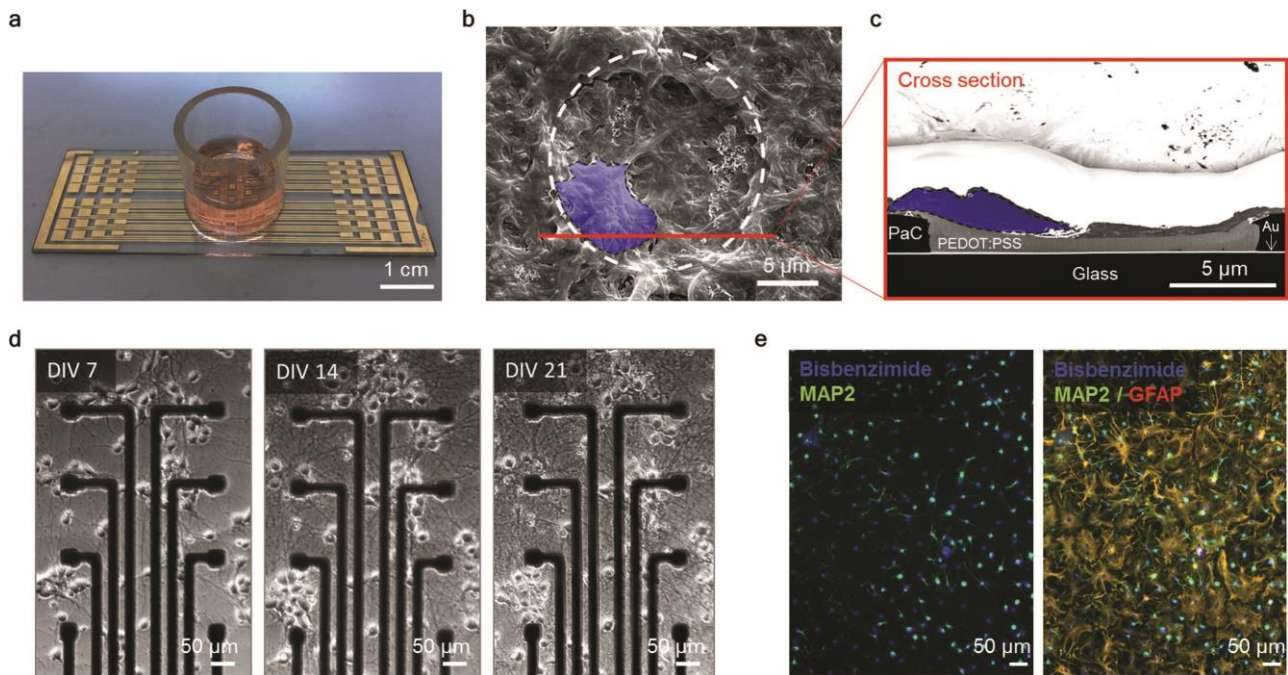


Figure 1. Presentation of the MEA device and primary cell culture thereon. a) Photograph of the parylene-insulated and PEDOT:PSS-coated MEA. A glass well is attached as container for the cell culture. b) SEM image of a top view of a microelectrode with a single cell adhered to the PEDOT:PSS. The white-dashed circle shows the boundary of the microelectrode, the blue area indicates the single cell, and the red line points out the location of the cut performed with FIB for the cross-section in (c). c) FIB-SEM image of a cross-section indicated in (b). The cell tightly adhered to the PEDOT:PSS-coated microelectrode. d) Phase contrast images of the cortical cell culture at DIV7, 14, and 21 showing the growth of the cells on the MEA. e) Immunofluorescence analysis of rat E18 primary cortical cells on parylene C-coated glass substrates. Neurons were stained for MAP2 (green), astrocytes for GFAP (orange), and cell nuclei with bisbenzimidazole (blue). Abbreviations used: PaC, Parylene C. Au, gold.

confirmed at DIV21 through an immunofluorescence analysis (Figure 1e). Neurons were stained for the neuronal marker Microtubule associated protein 2 (MAP2, green), astrocytes for the Glial fibrillary acidic protein (GFAP, orange) and all cell nuclei for bisbenzimidazole (blue). Both cell types were homogeneously spread on the surface. The astrocytes were clearly visible in between the smaller cell-bodied neurons, playing their essential role of neuronal support.^[15,16] A serum-free media were used without any growth factors to prevent astrocytes from further proliferation. The cells showed a very high survival rate at DIV21 on the PDL- and laminin-coated MEAs (Figure S2e, Supporting Information).

in one particular color. In Figure 2a, this means that 3 different neurons were detected at LCD, and 12 neurons were detected at HCD. HCD on MEAs therefore resulted in the recording of significantly more neurons.

To show more clearly the difference between the recordings of LCD and HCD, recordings from single electrodes of both experimental groups are shown in Figure 2b. The recording graphs present the amplitude of the recorded signal in voltage as a function of time. Raster plots are shown just below, which indicate the occurrence of single units in time from one or

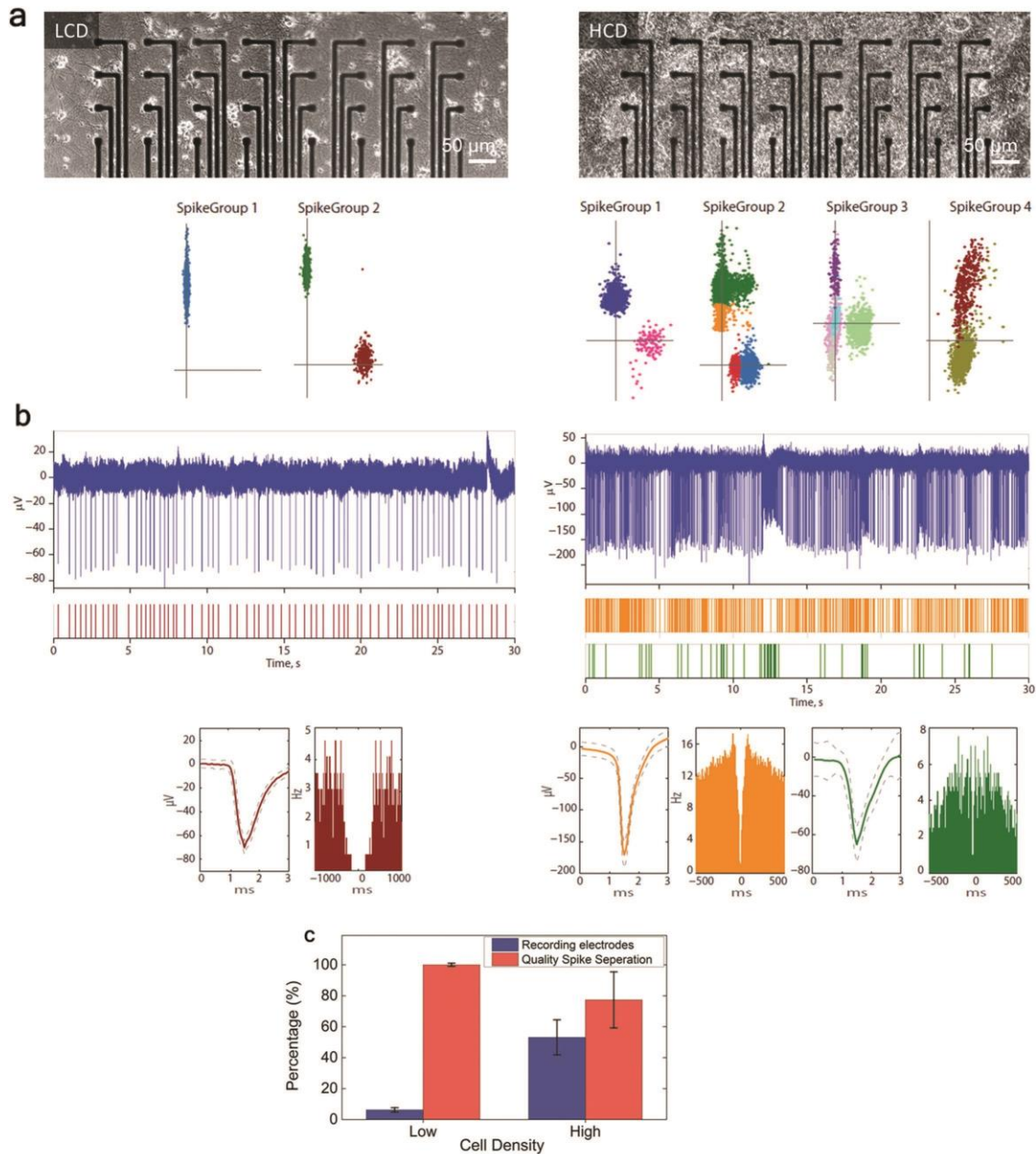


Figure 2. The influence of cell density on MEA recordings. a) Phase contrast images and PCA-based scatter plots of (left) LCD ($500 \text{ cells mm}^{-2}$) and (right) HCD (900 cell mm^{-2}). The scatter plots display the “clustering” of the single units into isolated clusters (individual neurons) in the principal component space, which are represented by different colors. More single unit activity was recorded at HCD compared with LCD. b) Example of electrophysiological recordings with corresponding raster plot, unit waveforms, and auto-correlograms add parentheses (ACGs) per cell density group. c) Percentage of recorded electrodes and the quality of spike separation per cell density group. Data are presented as mean \pm SD ($n = 2$ per experimental group).

more neurons detected in that given signal. There are several observations from this result. First, the average recorded unit activity is higher in amplitude at HCD (Figure S2, Supporting Information). It is well known that unit activity is mostly the extracellular summation of recorded signals from the neural somas and proximal dendrites.^[12] Moreover, the voltage amplitude mostly depends on the proximity of the neural soma to the electrode sites, decreasing rapidly with increasing distance from the electrode.^[12,26] The highest amplitudes were found at higher cell density, which implies that those cells were more likely to be located proximal to the electrodes. This can be explained by the larger number of cells that is present on the MEA,

increasing the probability of cell bodies positioned closer to the electrode site. Second, the recorded activity of single electrodes at HCD contained activity of multiple neurons, unlike the recordings at LCD (Figure 2b, raster plots). This means that a single electrode can pick up more signals at HCD compared with LCD, which stands to reason as the probability of their location near a given recording site would increase. The capability of recording from cultures with higher density is important as it moves the device performance in the direction of the higher density packing of neurons observed in tissue in the brain.

Despite a clear increase in unit recordings at HCD in vitro, the complexity of spike sorting increased (Figure 2b,c). Below the

recordings of Figure 2b, an example is given of detected waveforms of single units and their autocorrelograms (ACG). These graphs show the voltage amplitude and frequency of the signal as a function of time, respectively. A clear refractory period was observed in the ACG of LCD groups, which means that the probability that the sorted units belong to a single neuron is very high. This was however not always the case for HCD ACGs. This is a plausible consequence of having many more cells on or near the electrode sites at HCD emitting units simultaneously. Thus, there is a small trade-off between number of recording electrodes and spike separation quality. However, the increase in recording electrodes at HCD ($53.10\% \pm 11.31\%$ at HCD vs $6.25\% \pm 1.41\%$ at LCD) by far outweighed the small decrease of signal separation ($77.30\% \pm 18.00\%$ vs $100\% \pm 0.00\%$).

2.3. The Formation of Neurospheres

The significant enhancement of recordings at HCD led us to consider a more 3D organization of the primary cell culture on MEAs. Since a more compact cell culture increased the probability of recordings, we reasoned that it might be beneficial to engineer highly local clusters in cell density, commonly known as neurospheres.^[27] Previous work has reported stimulation of

neurospheres^[28] and the network bursting activity of neurospheres.^[29-31] However, in this work, we focus on single unit activity and do not use any surrounding scaffold or supporting structure to facilitate 3D tissue formation.^[32] We anticipated that this would result in more electrophysiological recordings as more cells are expected in closer proximity to the microelectrodes, especially in the z-direction. Moreover, cells would be positioned closer to other cells, forcing them to form neurites in many more directions.

The formation of neurospheres with primary E18 cortical cells was observed at HCD using NbActiv4 media. **Figure 3a** shows that neurons are present in the neurosphere on parylene-coated glass slides used as control samples. As previously mentioned, neurons, astrocytes, and cell nuclei were stained for MAP2 (green), GFAP (orange), and bisbenzimid (blue), respectively. A live/dead assay was performed on DIV21 to show the survival of cells within the neurosphere (Figure 3b). The same neurosphere formations were subsequently observed on MEAs, and some clusters fortuitously developed on top of microelectrodes (Figure 3c).

As anticipated, neurospheres on top of the microelectrodes significantly increased single unit recordings. The PCA-based scatter plot in Figure 3c gives an example of the units recorded from a single electrode, unlike previously shown, on the MEA covered with a neurosphere. The six different colors show the unit activities of six different neurons. The unit waveforms and ACGs of these

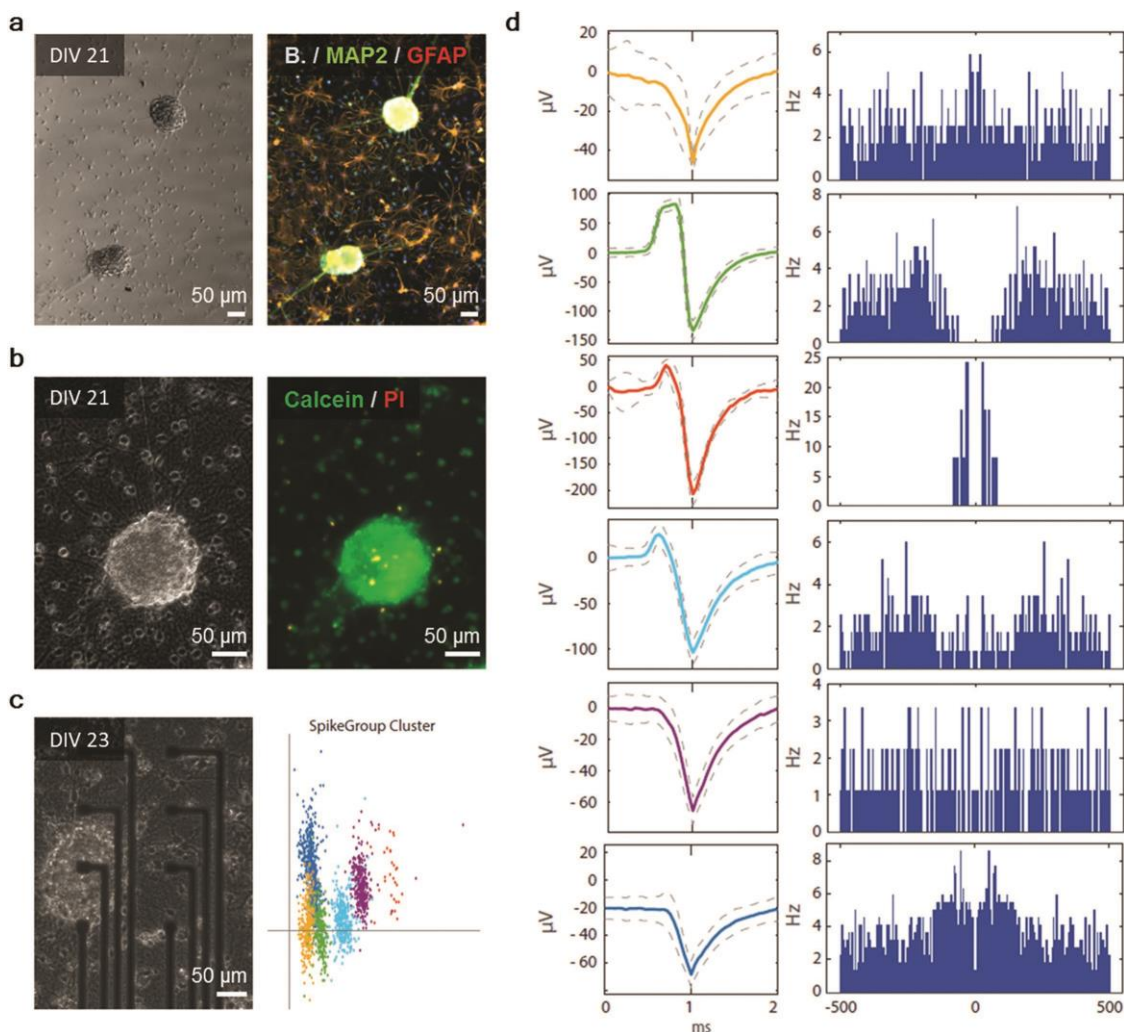


Figure 3. Neurospheres increase the number of single unit recordings on a single microelectrode. a) Phase contrast image and fluorescence image of cells on DIV21 seeded on parylene-covered glass slides (control samples) at HCD, cultured in NbActiv4. b) Phase contrast image and corresponding fluorescence image of live/dead staining on DIV21. Green cells are alive (calcein) and dead cells are orange (propidium iodide). c) Phase contrast image of a neurosphere on top of a microelectrode at DIV23 and the PCA-based scatter plot showing the unit detection of 6 different neurons from the recorded electrophysiology on that single electrode. d) The corresponding single unit waveforms and ACGs of the six different neurons. Abbreviations

detected neurons are shown in Figure 3d. Detection of up to seven neurons with a single microelectrode was achieved. This multineuron recording with a single electrode had not previously been observed. In total, 76 different neurons were detected with 45 microelectrodes containing neurospheres on the top. Moreover, the overall chance of recording increased with the presence of neurospheres. While only 3 microelectrodes with single cells on and around microelectrodes resulted in successful recordings ($2.4\% \pm 0.7\%$ out of 123 microelectrodes recorded on a total of five MEAs), 45 microelectrodes with neurospheres on top successfully measured single unit activity ($44.6\% \pm 8.5\%$ recorded of 101 microelectrodes on a total of 5 MEAs). The success rate of recording single unit activity per microelectrode has thereby increased with more than 40%.

A high level of interconnectivity was observed between the neurospheres on the MEAs (Figure 4). The cell distribution was investigated at DIV21 on a parylene-coated glass slide to avoid limitation from the metal MEA pattern. While neurons seem to predominate in the neurosphere (Figure 4a-c), a selection of z-stack images showed that astrocytes were also located within (Figure 4d). Interestingly, despite the 3D organization of the cells on a 2D device, neurons above the plane of the MEA managed to extend processes down to make connections with the substrate surface (Figure 4e-g). The neurospheres were aggregations of cells with heights of up to at least $100\ \mu\text{m}$. Thick bundles of neurites from various orientations on the sphere were observed radiating out to connect with neighboring neurospheres and attached at different

points on the MEA. This observation could indicate that recordings were not necessarily limited to the cells in direct contact with the electrode site, but also from neurons located at higher positions on neurospheres.

2.4. Laser Patterning of PEGDA to Control Positioning of Neurospheres

UV-photocrosslinking has been used extensively for in vitro studies as an effective approach for the formation of polymeric structures for cell patterning.^[33,34] In contrast to other photopolymerization patterning techniques, laser writing is a direct process, which offers great versatility and the capability to precisely create microscale features on various surfaces. Given the success of recording from neurons when neurospheres were proximal to electrodes, attempts were made to control the placement of the neurospheres on the MEA with an antifouling region around the electrode sites. To achieve this, a PEGDA solution was deposited on top of the MEA through doctor blading and subsequently irradiated by a UV (343 nm) laser beam. The resulting topographic pattern consisted of separate PEGDA lines with a width of $\approx 12\ \mu\text{m}$ and an interspacing of $40\ \mu\text{m}$, as shown in Figure 5a. It should be noted that the dimensions and the characteristics of the pattern were chosen in relation to the size of the neurosphere and the position of the electrodes in our MEA design

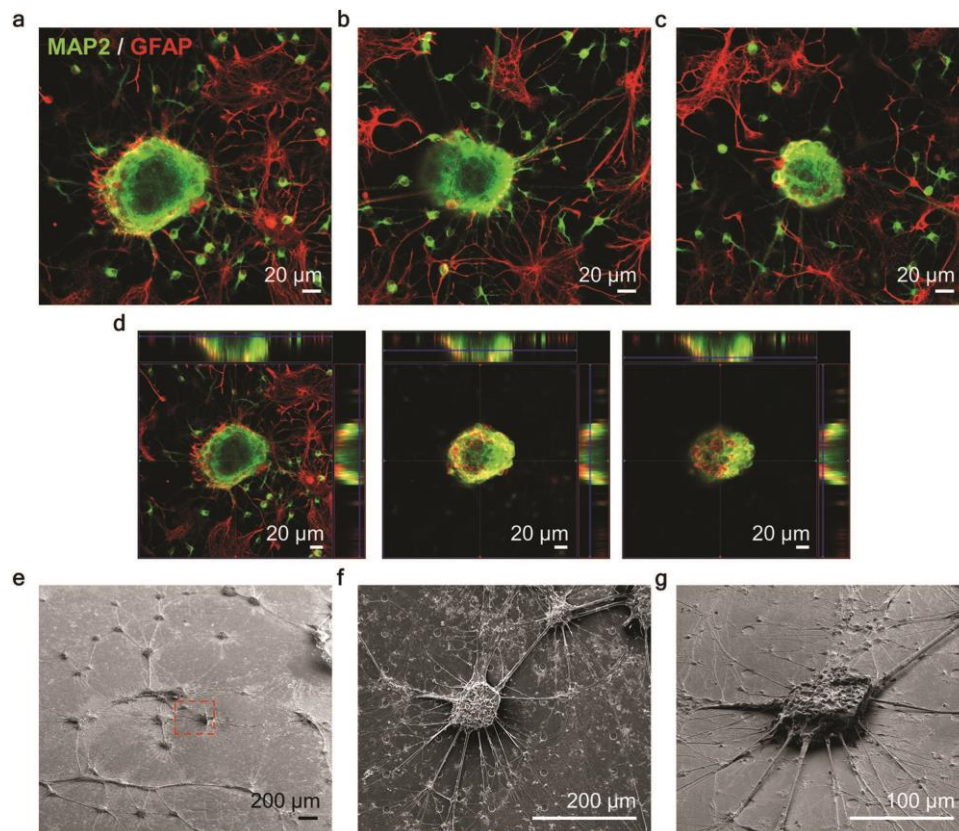


Figure 4. Optical characterization of the neurospheres. a-c) Confocal fluorescence images of neurons (MAP2, green) and astrocytes (GFAP, red) of various neurospheres on parylene-coated glass slides. Neurons were observed within the neurosphere, closely surrounded by astrocytes. d) A selection of z-stack images from (a), starting at the substrate plane (left) and moving to more upward planes (right). Individual small neurons and large astrocytes are observed on the surface of the substrate. Both cell types are clearly visible within the neurosphere. SEM images of neurospheres adhering to the MEA. e) Overview of the 3D organization of the primary cell culture. Multiple large neurospheres are formed on the substrate. The red-dashed box shows the array section that is further visualized in (f-g). f) Top and g) tilted view on neurospheres tightly adhered to the MEA. Neurons above the MEA plane extended processes down to the MEA, thereby connecting to neighboring neurospheres, individual cells and the microelectrodes.

PEGDA is known to exhibit poor adhesion properties for cells due to limited protein adsorption on its surface.^[35,36] Figure 5b,c depicts a neurosphere at DIV21 being confined within the region defined by the PEGDA lines, which is successfully patterned on top of the microelectrode. The laser-patterned PEGDA structures not only allowed us to place the neurospheres on top of the electrode sites, it also provided guidance

of neurite outgrowth toward neighboring electrodes and neurospheres (Figure 5d-f). The orientation of the neurites was observed along the pattern and deviated only from these lines once other neurospheres were in close proximity (Figure 4d). In contrast, the astrocytes seemed to not have a particular distribution induced by the PEGDA pattern (Figure 5e).

The laser-patterned PEGDA structures contributed to the formation of large neurospheres, which consequently enabled the tracking of single unit activity on neighboring electrodes (Figure 6). Figure 6a shows a neurosphere located in the bottom right corner of the fluorescence image, almost fully covering two electrode sites (E2 and E3) and reaching out to a third electrode (E3) with its neurite network. Single unit activity of three different neurons was detected on all three electrodes (Figure 6b,c). The corresponding recordings (Figure 6c) and single unit waveforms from one neuron (Figure 6d) show a clear increase in amplitude from E1 to E3. This means that the neuron in question must be located in closer proximity to E3, while its electrical signal is simultaneously also recorded up to almost 200 μm further. This is in line with previously reported recording limit of well-isolated extracellular spikes.^[12] We thus show that we can reach similar electrophysiological recording limits with this PEGDA-induced neurosphere in vitro culture compared with those of actual in vivo recordings.

3. Conclusions

Overall, we showed successful in vitro MEA recordings with 48 electrodes out of a total of 224 ($n = 7$ MEAs). This is a recording yield of 21.4% from which 93.75% was obtained from electrodes with neurospheres and 6.25% from single cells on and around the microelectrodes. The 3D conformation of E18 rat primary cortical cells in neurospheres resulted in a significant improvement of MEA recording success. Through spike sorting algorithms, we showed how unit activity per microelectrode increased with HCD and with neurospheres. The presence of neurospheres on the MEA resulted in multineuron detection with a single microelectrode and allowed for simultaneous recording of single unit activity with neighboring electrodes. This enhanced recording yield on planar MEAs using a 3D neural in vitro model will facilitate pharmacologybased studies providing more electrophysiological data. The engineering of these highly local clusters of neurons and their processes by substrate patterning, is not unlike the organization of nuclei and their tracts in the brain, and shows promise for the potential of construction of minibrain structures on MEA devices.

4. Experimental Section

MEA Fabrication: The MEAs were fabricated as previously reported,^[11] containing 64 electrodes each with a $12 \times 12 \mu\text{m}^2$ recording area (Figure S1a, Supporting Information). The fabrication included the deposition and patterning of gold, parylene C and PEDOT:PSS on glass substrates. Substrates ($25 \times 75 \text{mm}^2$) were thoroughly cleaned by sonication steps of 10 min in a soap bath followed by bath mixture of acetone/ isopropanol (1:1). The clean substrates were spin coated with S1813 photoresist (Shipley) and exposed to UV light with a SUSS MJB4 contact aligner. A paper mask (Selba, S.A.) was used during exposure, after which the samples were developed in MF-26 developer. Chromium and gold were deposited in a metal evaporator with final thicknesses of 10 and 100 nm, respectively. Lift-off was done in a solvent bath of acetone/isopropanol (1:1). Then, two layers of parylene were

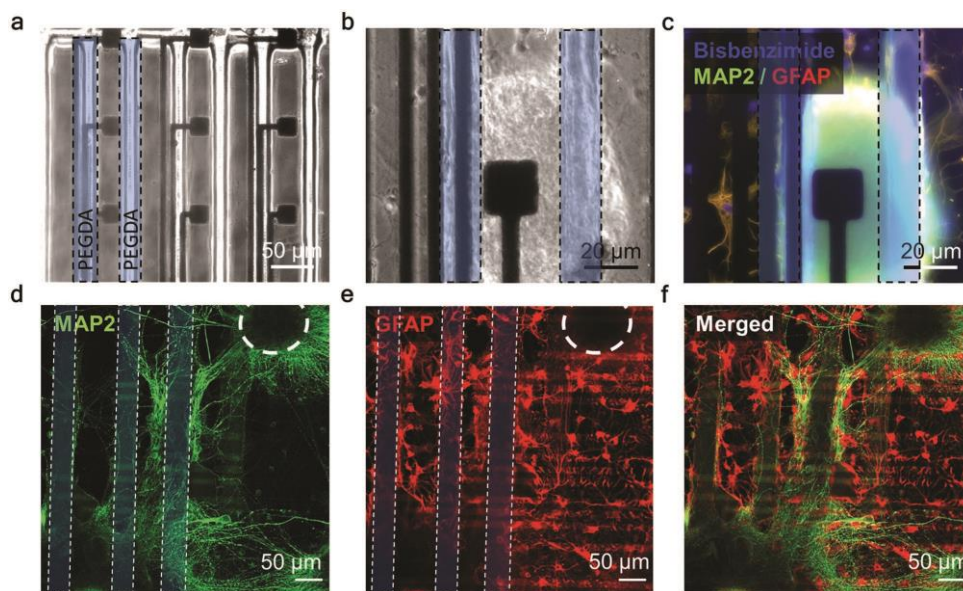


Figure 5. PEGDA patterning for more accurate control on neurosphere placement and neurite outgrowth. a) Phase contrast image of nine microelectrodes surrounded by a PEGDA pattern to confine cell adhesion. For clarification purposes, two PEGDA lines are shown in blue. b) Phase contrast image and c) fluorescence image of a neurosphere restricted by the PEGDA lines. Neurons, astrocytes, and cell nuclei are stained for MAP2 (green), GFAP (orange), and bisbenzimidide (blue), respectively. d-f) Confocal images of neurons (MAP2), astrocytes (GFAP), and its overlay showing the guidance of PEGDA lines for neurite outgrowth. PEGDA lines are shown in blue, while the striped pattern perpendicular to the PEGDA lines result from decreased transmission through the metal MEA lines. The boundaries of the neurospheres are illustrated with bold white-dashed lines.

deposited with a SCS Labcoater each with thickness of $\approx 2 \mu\text{m}$. During the first deposition, 3-(trimethoxysilyl)propyl methacrylate (A-174 Silane) was added to the deposition chamber as an adhesion promoter. Before the second parylene deposition, a sacrificial layer of soap (1% in deionized (DI) water, Micro-90) was spin coated. This created an antiadhesive layer to facilitate peel-off at a later stage. Photoresist AZ 9260 (Microchem) was then spin coated on the substrates, followed by another photolithography and

development step using AZ Developer. The parylene was etched to open the microelectrode areas through reactive ion etching using O_2 plasma (Oxford 80 Plasmalab plus). A PEDOT:PSS dispersion, including Clevis PH 1000 (Heraeus Holding GmbH), 5 wt% ethylene glycol, 0.1 wt% dodecyl benzene sulfonic acid, and 1 wt% of (3-glycidioxypropyl)trimethoxysilane), was spin coated on the devices, and the sacrificial second parylene layer was peeled off. Finally, the devices were hard baked at 140°C for 1 h and immersed in DI

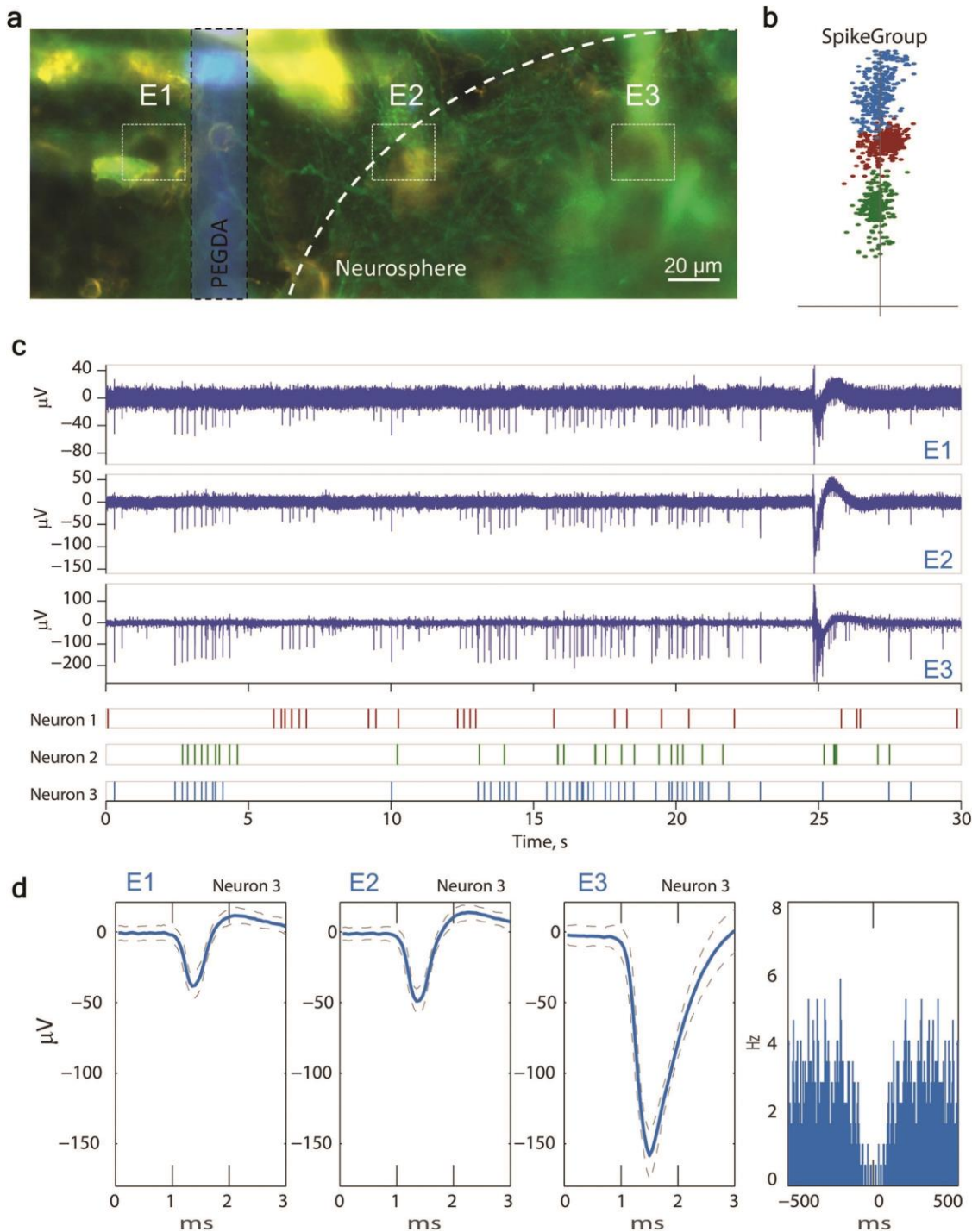


Figure 6. PEGDA patterning to track single unit activity on neighboring electrodes. a) Fluorescence image of a neurosphere covering almost three electrodes (E1-E3). The dashed white line illustrates the boundary of the neurosphere and the dashed white boxes indicate the location of the electrodes. b) PCA-based scatter plot, showing the detection of three different neurons from the recorded signals. c) Recordings of E1-E3 with corresponding raster plot of the detected neurons, showing an increase in voltage amplitude from E1 to E3. Recorded neurons are consequently in closer proximity to E3. d) Single unit waveforms of Neuron 3 recorded with E1-3 and the corresponding ACG.

water over night. This last step removed any excess of low molecular weight compounds inside the PEDOT:PSS dispersion.

MEA Preparation for Cell Culture: Protein Coating: Glass wells with an inner diameter of 3 cm² were attached to the MEAs using polydimethylsiloxane (PDMS) as glue. The devices were plasma treated at 25 W for 1 min to make the surface hydrophilic for cell culture. The inside of the well was kept wet from this point on with DI water. The devices were entirely sterilized for 30 min in 70% ethanol and rinsed with Dulbecco's phosphate-buffered saline (DPBS). The devices were then coated with 50 µg mL⁻¹ PDL (70 kDa, Sigma Aldrich) in DI water for 2 h at 37 °C, rinsed three times with DPBS and left overnight in DPBS at 37 °C. Next, the devices were coated with 20 µg mL⁻¹ of laminin (Sigma Aldrich) in DPBS for again 2 h at 37 °C, rinsed three times with DPBS and were placed in the incubator with fresh DPBS until cell seeding.

Laser Patterning PEGDA via Photopolymerization: Prior to the laser writing process, the substrates were functionalized for the covalent bonding of PEGDA ($M_n = 575$). 3-(Trimethoxysilyl)propyl methacrylate (A-174 Silane, Sigma Aldrich) was deposited by chemical vapor deposition under vacuum for 2 h at 90–100 °C to provide ClC moieties for efficient PEGDA adhesion. 2-Hydroxy-2-methylpropiophenone (>98%, Sigma Aldrich) was incorporated as a photoinitiator and mixed with PEGDA:water solution (1:1) at a concentration of 0.5 wt%. The solution was spread onto the substrates using a handheld doctor blade and placed in the substrate holder for laser processing. The system used for the direct laser writing of PEGDA was based on a subpicosecond laser source coupled to a laser scanning head. A femtosecond-diodepumped ytterbium amplified laser (Amplitudes Systems S-Pulse HP) was used with a fundamental wavelength of 1030 nm, while for the present experiments the third harmonic of 343 nm was used, after frequency conversion in nonlinear crystals. The pulse duration was set to 500 fs full width at half maximum, estimated from single-shot autocorrelation trace. The laser power was adjusted externally with a set of half waveplate and polarizer for each wavelength. The beam was focused on the sample after passing through galvomirrors (Thorlabs GVS12) and an f-Theta lens that depends on the wavelength: focal length of 254 mm (Thorlabs FTH254-1064) for the infrared and 100 mm for the UV (63-312, Edmund Optics). For the described experiments, the repetition rate of the laser was operated at 400 Hz, and the galvomirrors were synchronized with the laser, meaning that only one shot per location was done in case of a single pass. Homemade software was used for the control of beam displacements on the sample for a particular pattern. At 343 nm, the step size was found to be 8 µm, resulting in a beam overlap of more than 80%. A calibration of the energy in the sample plane was done with a calibrated pyroelectric sensor (OPHIR PE9-C) so that the local fluence can be estimated. After the laser irradiation, the samples were immersed into water for 5 min in order to remove the noncrosslinked parts from the surface and a protein coating was performed, as previously described.

Electrical Characterization: Impedance measurements were performed with a potentiostat (Autolab PGSTAT128N) in a three-electrode configuration. An Ag/AgCl electrode was used as the reference electrode, a Pt electrode was the counter electrode with the recoding electrode of the MEA was the working electrode. The characterization was performed in DPBS solution.

Cortical Cell Culture: E18 rat cortical tissues were purchased from Brainbits (Brainbits, LLC). The cells were dissociated with a 2 mg mL⁻¹ papain solution (Hibernate E-Ca without B27, Brainbits, LLC) for 10 min in a water bath at 30 °C. They were then triturated in Hibernate E containing 2% B27 and 0.5×10^{-3} m Glutamax (Hibernate EB media, Brainbits, LLC) to disperse most of the tissue, spun at 200 G for 1 min and resuspended in NbActiv1 media (Brainbits, LLC). Cells were plated at two cell densities, an LCD of 500 cells mm⁻² and a HCD of 900 cells mm⁻². Cell counting was performed using an aliquot of the cell suspension in a hemocytometer. The cells were cultured in NbActiv1 media, a serum-free B27/neurobasal media (Brainbits, LLC), at 37 °C in 5% CO₂-humidified incubators. Every 3–4 d, half of the media was replaced by fresh media. For the formation of neurospheres, NbActiv1 was replaced by NbActiv4, which additionally contains creatine, cholesterol, and estrogen.^[22]

SEM and FIB-SEM: All the cell cultures on the MEAs were washed three times with prewarmed DPBS and fixed with 3.5% glutaraldehyde overnight after DIV23. For the cross-sectional images, the cells were further processed with a ROTO staining, uranyl acetate, dehydrated, and embedded as presented in ref. [21]. Cross-sections were made and polished, fixing a voltage at 30 kV and current at 80 pA. A more detailed description of the FIB-SEM procedure is given in ref. [21]. Image acquisition of the cross-section was performed with a backscattered detector at 3–10 kV and at variable currents. For the neurosphere SEM images, the neurosphere cultures were dried in air, and gold was sputtered with a final thickness of 10 nm. The prepared arrays

were then mounted on SEM stubs with colloidal silver paste (TED PELLA). Images were acquired fixing a voltage from 3 to 15 kV with variable currents (secondary electrons detector).

Immunofluorescence Staining: Neurons were stained for the neuronal marker MAP2 (green), astrocytes for the glial marker GFAP (orange), and all cell nuclei with bisbenzimidazole (blue). The cells were fixed for 10 min in 4% paraformaldehyde (PFA)/0.12 m sucrose with 0.1% glutaraldehyde, followed by 2 rinsing steps with DPBS (without CaCl₂ and MgCl₂). The blocking/permeabilization step was done with 0.5% TritonX-100 and 5% BSA in DPBS for 5 min at room temperature. Mouse monoclonal antibody MAP2 (Life Technologies SAS) and rabbit monoclonal antibody GFAP (Millipore) were added at a 1:400 dilution in DPBS with 0.05% TritonX-100 and 5% BSA, for overnight at 4 °C. After 4 washing steps with DPBS, Alexa Fluor 488 donkey antimouse IgG (Abcam) and Alexa Fluor 568 donkey antirabbit IgG (Abcam) were added at a 1:500 dilution in DPBS with 0.05% TritonX-100 and 5% BSA for

1 h at room temperature. One wash with DPBS was followed by nuclear staining with a 1 µg mL⁻¹ bisbenzimidazole (Sigma Aldrich, 14533) solution. After washing, samples were examined with a fluorescent microscope (Zeiss Axio Observer Z1 Carl) and a confocal microscope (Zeiss SLM 800). All acquisition and processing was performed using ZEN Blue 2.3 lite software.

Live/Dead Staining: Live/dead assays were performed to examine cell viability on the different substrates. Cells were incubated in DPBS with ≈0.2 µg calcein AM and 0.3 µg propidium iodide for 10 min. Living cells were stained with green fluorescent calcein, due to the enzymatic cleavage by esterase of nonfluorescent calcein AM. Metabolic activity was required to enable this conversion, which was only possible in living cells. Dead cells were stained with a cell-impermeable propidium iodide, which binds to nucleic acids in the nucleus if the cell is dead.

Electrophysiological Recordings: Extracellular recordings were performed in a Faraday cage at high room temperature DIV23. All data were recorded with a 32-channel amplifier board (RHD2132, Intan technologies, US). This board was connected to MEAs via pogo pins held in place in a custom-made 3D printed holder, as previously reported.^[11] The sampling rate was 20 kHz.

Spike Sorting Analysis: Single unit activity was identified and isolated using the Neurosuite software package of Neuroscope, NDManager, and Klusters.^[23] First, spike groups were defined by grouping a maximum of eight electrodes, since a single neuron can potentially be seen by several electrodes.^[23,37] Then, for each spike group, the wide-band signals were highpass filtered at 300 Hz. The detection parameters were primarily optimized for the measured recordings and kept constant for all shown data. Single units were subsequently extracted at a threshold factor of 1.8 with a refractory period of 16 samples. After extracting the spikes from the raw signal, PCA allowed to extract the relevant components (three principal components per electrode) that retained most of the spike information. Then, the automatic spike-sorting algorithm KlustaKwik (<https://klustakwik.sourceforge.net>,^[25]) was used to tentatively assign the detected spikes to individual neurons. Finally, all the spike clusters were manually refined with Klusters.^[23] The spike separation quality was determined to be high when the isolated unit clusters showed a clear refractory period (Figure 2c). Data were subsequently plotted using custom-written tools in Matlab (Mathworks) and is presented herein as mean ± SD.

Supporting Information

Supporting Information is available from the Wiley Online Library or from the author.

Acknowledgements

The authors thank the Marie Curie initial training network OLIMPIA (Project No. 316832) for the financial support. The authors declare no competing financial interest. F.S. thanks Dr. Francesco de Angelis, Dr. Michele Dipalo, and Dr. Valentina Mollo (Italian Institute of Technology) for their help during SEM/FIB experiments.

Conflict of Interest

The authors declare no conflict of interest.

Keywords

bioelectronics, conducting polymers, electrophysiology, MEAs, primary cortical cells

Received: August 21, 2017
Revised: September 22, 2017
Published online:

References

- [1] World Health Organization, WHO Press, Geneva, Switzerland **2007**.
- [2] A. D. Gilmour, A. J. Woolley, L. A. Poole-Warren, C. E. Thomson, R. A. Green, *Biomaterials* **2016**, *91*, 23.
- [3] G. Buzsáki, C. A. Anastassiou, C. Koch, *Nat. Rev. Neurosci.* **2012**, *13*, 407.
- [4] M. E. J. Obien, K. Deligkaris, T. Bullmann, D. J. Bakkum, U. Frey, *Front. Neurosci.* **2015**, *8*, <https://doi.org/10.3389/fnins.2014.00423>.
- [5] M. E. Spira, A. Hai, *Nat. Nanotechnol.* **2013**, *8*, 83.
- [6] J. Pine, *J. Neurosci. Methods* **1980**, *2*, 19.
- [7] R. Kim, S. Joo, H. Jung, N. Hong, Y. Nam, *Biomed. Eng. Lett.* **2014**, *4*, 129.
- [8] S. Venkatraman, J. Hendricks, Z. A. King, A. J. Sereno, S. Richardson-Burns, *IEEE Trans. Neural Syst. Rehabil. Eng.* **2011**, *19*, 307.
- [9] M. Sessolo, D. Khodagholy, J. Rivnay, F. Maddalena, M. Gleyzes, E. Steidl, B. Buisson, G. G. Malliaras, *Adv. Mater.* **2013**, *25*, 2135.
- [10] Y. Furukawa, A. Shimada, K. Kato, H. Iwata, K. Torimitsu, *Biochim. Biophys. Acta* **2013**, *1830*, 4329.
- [11] D. A. Koutsouras, A. Hama, J. Pas, P. Gkoupidenis, B. Hivert, C. Faivre-Sarrailh, E. Di Pasquale, R. M. Owens, G. G. Malliaras, *MRS Commun.* **2017**, *7*, 259.
- [12] G. Buzsáki, *Nat. Neurosci.* **2004**, *7*, 446.
- [13] Y. Nam, B. C. Wheeler, *Crit. Rev. Biomed. Eng.* **2011**, *39*, 45.
- [14] Y. Nam, B. C. Wheeler, in *2nd Int. Conf. of the IEEE on Neural Engineering (EMBS)*, IEEE, Arlington **2005**, p. 325.
- [15] S. B. Achour, O. Pascual, *Neurochem. Res.* **2012**, *37*, 2464.
- [16] B. C. Wheeler, G. J. Brewer, *Proc. IEEE Inst. Electr. Electron. Eng.* **2010**, *98*, 398.
- [17] W. L. C. Rutten, T. G. Ruardij, E. Marani, B. H. Roelofsen, *Appl. Bionics Biomech.* **2006**, *3*, 1.
- [18] A. Blau, *Curr. Opin. Colloid Interface Sci.* **2013**, *18*, 481.
- [19] S. M. Ojovan, M. McDonald, N. Rabieh, N. Shmuel, H. Erez, M. Nesladek, M. E. Spira, *Front. Neuroeng.* **2014**, *7*, <https://doi.org/10.3389/fneng.2014.00017>.
- [20] S. G. Turney, P. C. Bridgman, *Nat. Neurosci.* **2005**, *8*, 717.
- [21] F. Santoro, W. Zhao, L. M. Joubert, L. Duan, J. Schnitker, Y. Burgt, H. Y. Lou, B. Liu, A. Salleo, L. Cui, Y. Cui, B. Cui, *ACS Nano* **2017**, *11*, 8320.
- [22] G. J. Brewer, T. T. Jones, M. D. Boehler, B. C. Wheeler, *J. Neurosci. Methods* **2008**, *170*, 181.
- [23] L. Hazan, M. Zugaro, G. Buzsáki, *J. Neurosci. Methods* **2006**, *155*, 207.
- [24] R. Quian Quiroga, *Scholarpedia* **2007**, *2*, 3583.
- [25] K. D. Harris, D. A. Henze, J. Csicsvari, H. Hirase, G. Buzsáki, *J. Neurophysiol.* **2000**, *84*, 401.
- [26] G. Buzsáki, E. Stark, A. Berényi, D. Khodagholy, D. R. Kipke, E. Yoon, K. D. Wise, *Neuron* **2015**, *86*, 92.
- [27] L. Hoelting, B. Scheinhardt, O. Bondarenko, S. Schildknecht, M. Kapitza, V. Tanavde, B. Tan, Q. Y. Lee, S. Mecking, M. Leist, S. Kadereit, *Arch. Toxicol.* **2013**, *87*, 721.
- [28] K. Okita, M. Kato-Negishi, H. Onoe, S. Takeuchi, in *26th Int. Conf. of the IEEE in Micro Electro Mechanical Systems (MEMS)*, IEEE, Taipei, Taiwan **2013**, p. 221.
- [29] M. Mayer, B. Müller, S. Kadereit, S. Ritter, C. Thielemann, *APPA Health* **2014**, *1*, 305.
- [30] M. Frega, M. Tedesco, P. Massobrio, M. Pesce, S. Martinoia, *Sci. Rep.* **2015**, *4*.
- [31] J. L. Bourke, A. F. Quigley, S. Duchi, C. D. O'Connell, J. M. Crook, G. G. Wallace, M. J. Cook, R. M. I. Kapsa, *J. Tissue Eng. Regen. Med.* **2017**, <https://doi.org/10.1002/term.2508>.
- [32] X. M. Ma, J. Elisseeff, *Scaffolding in Tissue Engineering*, CRC Press, USA **2005**.
- [33] Y. Wang, G. T. Salazar, J.-H. Pai, H. Shadpour, C. E. Sims, N. L. Allbritton, *Lab Chip* **2008**, *8*, 734.
- [34] Y. Gao, J. Broussard, A. Haque, A. Revzin, T. Lin, *Microsyst. Nanoeng.* **2016**, *2*, 15045.
- [35] E. K. U. Larsen, M. B. L. Mikkelsen, N. B. Larsen, *Biomicrofluidics* **2014**, *8*, 064127.
- [36] M. Peter, P. Tayalia, *RSC Adv.* **2016**, *6*, 40878.
- [37] P. Bartho, H. Hirase, L. Monconduit, M. Zugaro, K. D. Harris, G. Buzsáki, *J. Neurophysiol.* **2004**, *92*, 600.